New insight into the structural, electrochemical and biological aspects of macroacyclic Cu(II) complexes derived from S-substituted dithiocarbazate schiff bases

May Lee Low, Laure Maigre, Mohamed Ibrahim M. Tahir, Edward R. T. Tiekink, Pierre Dorlet, Régis Guillot, Thahira Begum Ravoof, Rozita Rosli, Jean-Marie Pagès, Clotilde Policar, et al.

X-ray and Solution Structure of Copper(II) Macroacyclic Bis(dithiocarbazate): Influence on Their Redox Properties and Bioactivities

May Lee Low[a,b], Laure Maigre[c], Mohamed Ibrahim M. Tahir[a], Edward R. T. Tiekink[d] Pierre Dorlet[e], Régis Guillot[f], Thahira Begum Ravoof[a], Rozita Rosli[g,h], Jean-Marie Pagès[c], Nicolas Delsuc[b*], Clotilde Policar[b]* and Karen A. Crouse[a,i]*

[a]*Department of Chemistry, Universiti Putra Malaysia, 43400 Serdang, Selangor (Malaysia), Fax: +6 03 89435380*; E-mail: kacrouse@gmail.com

[b]*École Normale Supérieure-PSL Research University, Département de Chimie, Sorbonne Universités - UPMC Univ Paris 06, CNRS UMR 7203 LBM, 24, rue Lhomond, 75005 Paris, (France)*, Fax: +33 1 44 32 24 02; E-mail: clotilde.policar@ens.fr ; nicolas.delsuc@upmc.fr

[c]*UMR-MD1, Aix-Marseille Université, IRBA, 27 boulevard Jean Moulin, 13385 Marseille (France)*

[d]*Department of Chemistry, University of Malaya, 50603 Kuala Lumpur (Malaysia)*

[e]*Laboratoire Stress Oxydant et Détoxication, Institute for Integrative Biology of the Cell (I2BC), Université Paris- Saclay, CEA, CNRS, Université Paris-Sud, Bât 532 CEA Saclay, 91191 Gif sur Yvette cedex (France)*

[f]*Institut de Chimie Moléculaire et des Matériaux d'Orsay, Bât. 420 Université Paris-Sud, 91405 Orsay (France)*

[g]*Department of Obstetrics and Gynaecology, Universiti Putra Malaysia, 43400 Serdang, Selangor (Malaysia)*

[h]*UPM-MAKNA Cancer Research Laboratory, Institute of Bioscience, Universiti Putra Malaysia, 43400 Serdang, Selangor, (Malaysia)*

[i]*Cape Breton University, Sydney, Nova Scotia B1P 6L2 (Canada)*

Keywords: Dithiocarbazate / Schiff base / Macroacyclic tetradendate NNSS ligand / Copper complexes / Bioactivity/

Abstract

Copper(II) complexes synthesized from the products of condensation of S-methyl- and S-benzyldithiocarbazate (SMHDH2 and SBHDH2 respectively) with 2,5-hexandione have been characterized using various physico-chemical (elemental analysis, molar conductivity, magnetic susceptibility) and spectroscopic (infrared, electronic) methods. The structures of SMHDH2, its copper(II) complex CuSMHD, the related CuSBHD as well as the pyrrole byproduct SBPY have been determined by single crystal X-ray diffraction. In order to provide more insight into the behaviour of the complexes in solution, electron paramagnetic resonance (EPR) and electrochemical experiments were performed. The antibacterial and anticancer activities of both ligands and complexes were evaluated. The compounds, dissolved in 0.5% and 5% DMSO, showed a wide range of antimicrobial activity against 10 strains of Gram-positive and Gram-negative bacteria. Investigation of the effects of efflux pumps and membrane penetration towards the antibacterial activity are reported herein. The antiproliferation activity of the compounds was observed to be enhanced upon complexation. Both Cu complexes are strongly active against human breast adenocarcinoma cancer cell lines MDA-MB-231 and MCF-7.

43 **TOC diagram**

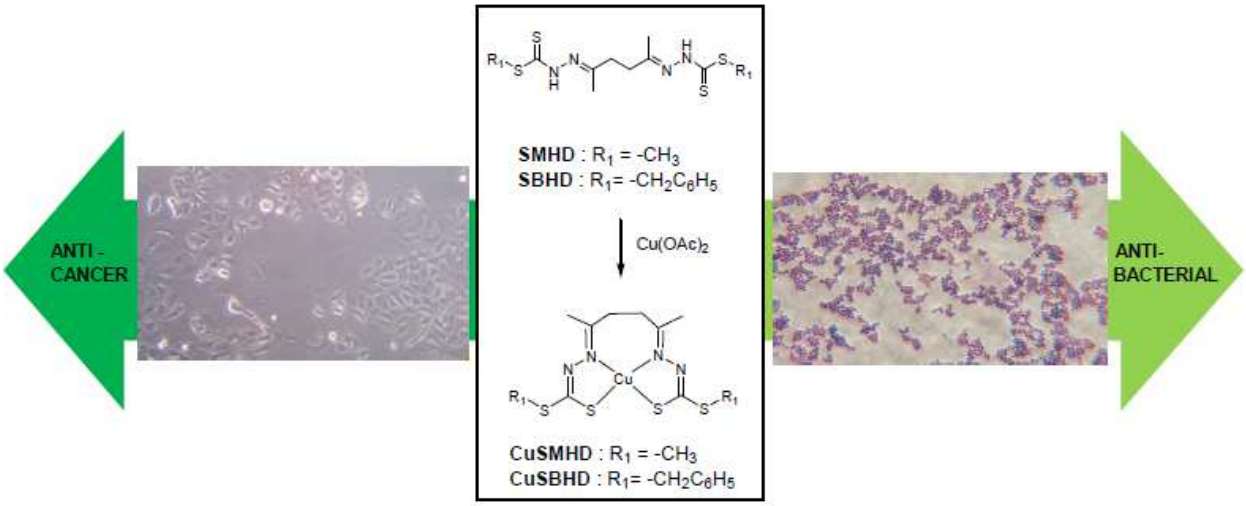

44

45

1. Introduction

Effective treatment of multi-drug resistant (MDR) bacterial infections has become increasingly challenging as the efficiency of the available antibiotic arsenal is reduced, resulting in increased frequency of therapeutic failure [1, 2]. One resistance pathway of MDR bacteria involves over-expression of efflux pumps, which expel structurally unrelated antibiotics causing a decrease in their intracellular concentration [3, 4]. It is essential to understand efflux-mediated resistance in bacterial pathogens to develop new antibacterial agents. In addition, parallel concerns relating to acquired drug resistance of current anticancer drugs as well as their serious side-effects in the midst of the increasing rate of cancer diagnoses, in particular breast cancer, drives the effort to develop better alternatives [5, 6]. Dithiocarbazate compounds with their plethora of potentially tunable biological activities are exciting candidates for exploration and development.

The sulphur-nitrogen chelating agents derived from S-alkyl/aryl esters of dithiocarbazic acid have been extensively investigated in recent years for their potential anticancer [7, 8], antibacterial [9], antiamoebic [10], anti-*Trypanosoma cruzi* [11] and anti-*Mycobacterium tuberculosis* [12] activities. Considerable attention continues to be given to these and related Schiff base ligands [13-16], since their properties can be modulated by introducing different substituents through condensation of various S-substituted dithiocarbazate esters with a wide array of aldehydes and ketones. In many cases, the biological properties of dithiocarbazate derivatives have been shown to be widely different although there may be only slight variation in their molecular structures [8]. Since these ligands possess both hard nitrogen and soft sulfur donor atoms they are capable of coordinating with a wide range of transition and non-transition metal ions forming metal complexes with interesting physicochemical and enhanced biological properties [17-19]. The wide diversity of structures displayed by macrocyclic and macroacyclic Schiff bases [20] result in various coordination abilities and lead to potential applications in biology ranging from therapeutics to diagnostics [21]. In addition, these compounds provide synthetic models for metalloproteins and metalloenzymes [22]. As part of our ongoing exploration of these interesting properties, we investigated the synthesis and characterization of some macroacyclic bis(dithiocarbazato) Schiff bases and their Cu(II) complexes in this work. The title compounds are analogues of the copper(II) bis(thiosemicarbazones) that have garnered much attention particularly as radiopharmaceuticals for the specific targeting of hypoxic tissue [23]. It was anticipated that

replacing nitrogen in thiosemicarbazones with sulphur might provide interesting results. 2,5-hexanedione was chosen to form the Schiff bases to enhance ligand flexibility, thereby facilitating increased tetrahedral distortion which could lead to incorporation of metal cations, such as Cu(I), that generally prefer non-square planar geometries [24]. It has been definitively shown that biological activity is related to the geometry at the metal site and, in the investigation of SOD mimics, it was noted that complexes with more pronounced tetrahedral distortion display higher activity [25, 26]. Copper complexes derived from thiosemicarbazate have been subjected to intensive research and appeared to be very efficient as antimicrobial [27] and anticancer [28] agents. The copper(II) complexes of NNSS ligands reported in the literature are also known to be neutral, stable ($K_{ass}=10^{18}$) compounds that easily cross cellular membranes [23, 29]. Thus, it is logical that copper ion serve as an excellent choice in our continuous search for effective metallodrugs.

The main aim of the present work is to explore the biological potential of Cu(II) bis(dithiocarbazate) complexes by determining their cytotoxicity and their potencies against different bacterial strains expressing a multi-drug resistance phenotype. Whereas syntheses of many dithiocarbazate compounds have been reported in the literature, there are only limited reports on the bioactivities [30], crystallography, EPR and electrochemistry [31, 32] with Cu(II) bis(dithiocarbazate). To promote effective bioactivities, it is essential to orient effort towards correlating the biological activities of this class of compounds with their solid and solution structures as well as their physico-chemical properties to identify the optimum geometry about the Cu ion. This goal can be achieved through the synthesis of a graduated series of ligands designed to reveal the mode of bioaction.

2. Results and Discussion

2.1. Synthesis and characterization

The synthesis of S-substituted dithiocarbazates was performed as previously described [33, 34]. Carbon disulfide and hydrazine were reacted in basic ethanol. After workup, the dithiocarbazate produced was directly reacted with methyl iodide or benzyl chloride to afford S-methyldithiocarbazate (SMDTC) and S-benzyldithiocarbazate (SBDTC), respectively. Schiff bases were then prepared by a slight variation of the method described by Ali *et al.* [35]. The respective S-substituted dithiocarbazates and 2,5-hexandione were condensed in 2:1 ratio (Scheme 1). The initial attempts to synthesize the ligand SBHDH2

(Scheme 2) with prolonged heating followed by purification using column chromatography were unsuccessful. NMR, ESI, elemental analysis and single crystal X-ray diffraction confirmed cyclization to the pyrrole derivative. We postulate that bis(dithiocarbazate) indeed formed but subsequently hydrolyzed to mono(dithiocarbazate) and S-benzyldithiocarbazate [36, 37] with subsequent cyclization of the mono(dithiocarbazate) to a pyrrole *via* the Paal-Knorr reaction. To our knowledge, this is the first pyrrole reported to be derived from a dithiocarbazate although there are two recent reports of formation of pyrrole byproducts upon reaction of thiosemicarbazone with 2,5-hexandione [38, 39]. Encouraged by the remarkable pharmacological properties of functionalized pyrrole [40, 41], we tested the compound for its antimicrobial activity, the results of which are discussed below. The Schiff base, SBHDH2, was finally obtained using either of the following two methods: stirring the dione and SBDTC at room temperature for 30 minutes or heating for only 5 minutes after which the white precipitate formed immediately. SMHDH2 was synthesized without the complication of side-reaction occurrence. The precipitate was recrystallized to afford pure SMHDH2 (70% yield).

Cu(II) complexes with NNSS coordination were obtained from the reaction of copper(II) acetate with equimolar amounts of the respective ligand (in acetonitrile for SBHDH2 and methanol for SMHDH2). The complexes were isolated by filtration with yields of 77% and 73% for CuSMHD and CuSBHD, respectively. Black crystals were grown from acetonitrile.

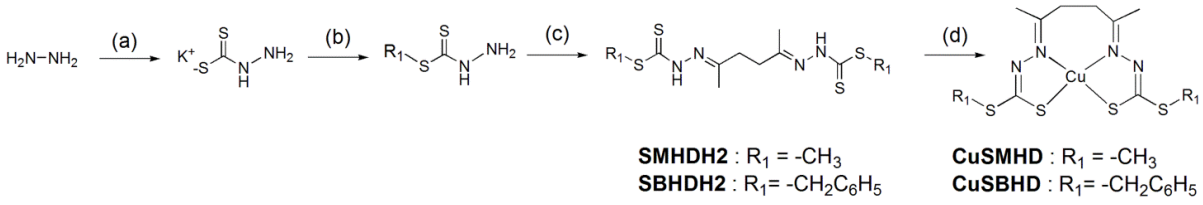

Scheme 1. Synthesis of the copper complexes derived from bis(dithiocarbazate) ligands. a) CS_2, KOH, EtOH, 0°C, 1 hour; b) CH_3I or $PhCH_2Cl$, EtOH, 0°C, 5 hr; c) for SMHDH2 (2,5-hexanedione, EtOH, 79°C, 1 hour), for SBHDH2 (2,5-hexanedione, EtOH, 79°C, 5 minutes) and d) for CuSMHD [$Cu(OAc)_2 \cdot H_2O$, MeOH, 65°C, 1 hour], for CuSBHD [$Cu(OAc)_2$, acetonitrile, r.t., 1 hour].

2.2. Characterization of the complexes in the solid state

The characteristic infrared band of the S-substituted dithiocarbazate ligand, ν(N-H) at *ca.* 3129 cm^{-1} and ν(C=S) at *ca.* 1050 cm^{-1} disappeared upon formation of the Cu(II) complexes confirming deprotonation of nitrogen to form the iminothiolate ion and its chelation through N and S. ν(C=N) of the azomethine bond shifted to lower energy (1611 cm^{-1} and 1606 cm^{-1} for CuSMHD and CuSBHD respectively. A second band due to ν(N=C) in complexes containing anionic dithiocarbazate moieties was also resolved [42]. The ligand hydrazinic band ν(N-N) at *ca.* 828 cm^{-1} also shifted upon complexation, to higher (CuSBHD) and lower (CuSMHD) wavenumbers. All these observations confirm deprotonation of the Schiff bases with coordination through the azomethine nitrogen atom. The ligand ν(CSS) band *ca.* 985 cm^{-1} split into two components at 1000-955 cm^{-1} upon complexation. The presence of this band and the absence of the C=S band in the spectra of the metal complexes provide additional evidence of the coordination of the Schiff base to the metal in its thiolate form [43, 44]. The complexes were also characterized by elemental microanalysis. The analytical data agree well with the formulations proposed for the complexes.

Magnetic susceptibility values at room temperature for the CuSMHD and CuSBHD complexes were determined using a Sherwood Magnetic Susceptibility Balance-AUTO to be 1.66 B.M and 1.48 B.M, respectively, as expected for paramagnetic $3d^9$ ions in a square-planar environment (spin-only value 1.73 B.M) [44, 45]. The slightly low values observed can be attributed to interaction between Cu(II) ion centers [46, 47]

As mentioned in synthesis and characterization, pyrrolyl derivative SBPY is a cyclisation product obtained during the attempted synthesis of SBHDH2. The molecular structure of SBPY is shown in Fig. 1a. In SBHDH2, the central CN_2S_2 chromophore is planar (r.m.s. = 0.0490 Å) and forms dihedral angles of 88.49(4) and 68.14(4)º with the pyrrolyl and phenyl rings, respectively. As the rings lie to the same of the molecule and opposite to the thione-S1 atom, the overall conformation is best described as being U-shaped. The dihedral angle between the rings is 60.874(6)º indicating a splayed relationship. The thione-S1 and amine-H atoms are syn which might be expected to lead to an eight-membered $\{\ldots HNCS\}_2$ synthon in the crystal packing. Nevertheless, the most prominent feature of the crystal packing is the formation of N–H…π (pyrrolyl) interactions, Fig. 1b, which lead to the formation of centrosymmetric dimeric aggregates.

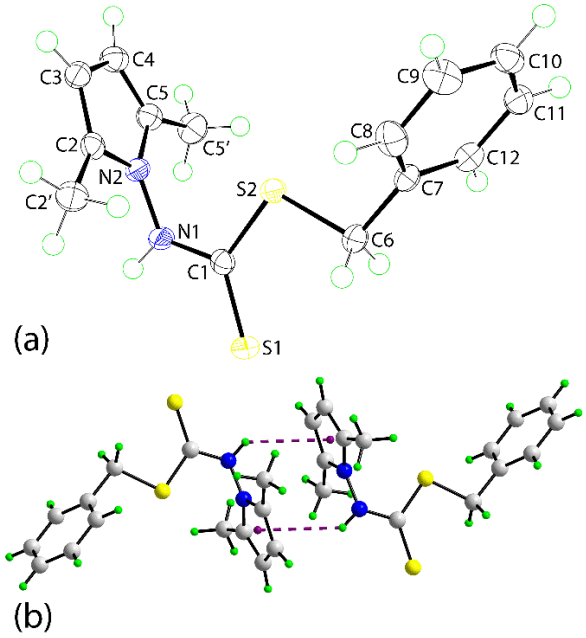

Fig. 1. (a) The molecular structure of SBPY, showing atom-labelling scheme, and (b) supramolecular dimer sustained by N–H…π (pyrrolyl) interactions.

The molecular structure of SMHDH2 crystallises about a crystallographic centre of inversion located at the mid-point of the C3-C3^{i} bond indicting the molecule has an anti disposition of the dithiocarbazate residues; symmetry operation i: 1-x, 2-y, 1-z. The conformation about the hydrazone bond is E. The entire molecule is planar with the r.m.s. for the 18 non-hydrogen atoms comprising the entire molecule being 0.038 Å, with the maximum deviations being ±0.061 Å for the S2 atom.

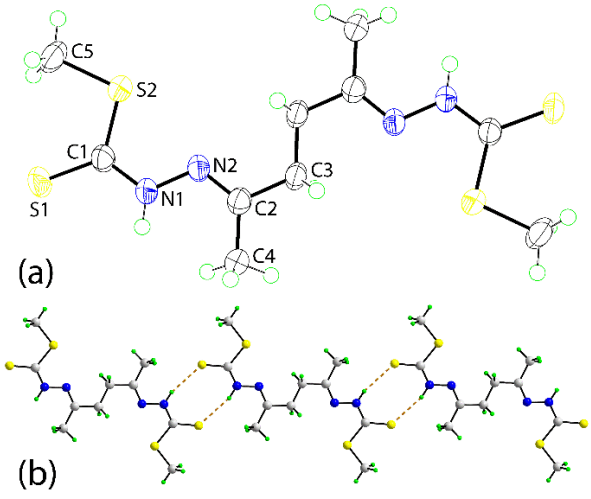

Fig. 2. (a) The molecular structure of SMHDH2, showing atom-labelling scheme. Unlabelled atoms are related by the symmetry operation 1-x, 2-y, 1-z, and (b) supramolecular chain mediated by N–H…S hydrogen bonds via centrosymmetric eight-membered {…HNCS}$_2$ synthons. [N1–H1n…S1 = 2.64(2) Å, N1…S1 = 3.455(2) Å, and angle at H1n = 156(3)º; symmetry operation i: 2-x, 2-y, 2-z]

The doubly deprotonated SMHD species functions as a tetradentate N_2S_2 donor ligand in its complex with copper(II). The molecular structure of CuSMHD is shown in Fig. 3a and selected geometric bond lengths (Å) and angles (°) for this, CuSBHD and for SMHDH2 are collected in Table 1. To a first approximation, the seven-membered ring may be described as having a half-chair conformation where the C4 atom lies 0.9317(16) Å above the plane defined by the Cu, N2, N3, C2, C3 and C5 atoms; r.m.s. = 0.1373 Å with maximum deviations 0.1590(6) Å for Cu and -0.1595(10) Å for C2. The two five-membered chelate rings have similar conformations. The S1-containing ring is an envelope with the flap atom being the Cu atom which lies 0.7857(16) Å above the least-squares plane defined by the remaining four atoms (r.m.s. = 0.0119 Å). By contrast, the S3-containing ring is considerably more planar but is still described as having an envelope conformation with the Cu atom being the flap. In this description, the Cu atom lies 0.2103(18) Å out of the plane defined by the four remaining atoms which has a r.m.s. of 0.0043 Å. There is a clear distortion away from the ideal square planar geometry as is commonly observed in seven-membered rings having two hydrazone bonds [48]. In CuSMHD, the angle between the two five-membered chelate rings is 46.10(2)º, and the range of angles subtended at the Cu atom is 84.89(3)º for S1–Cu–N2 to 164.90(4)º for S1–Cu–N3.

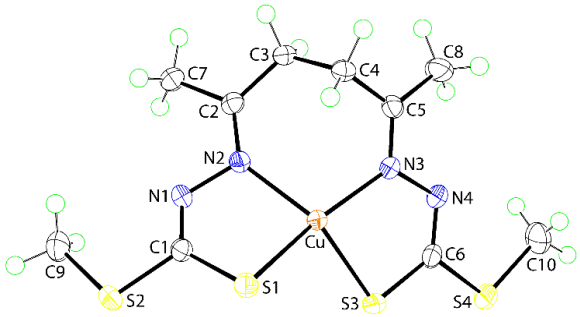

Fig. 3. The molecular structure of CuSMHD, showing atom-labelling scheme.

The availability of the crystal structure of SMHDH2 enables a comparison of the geometric parameters in the free molecule and in its coordinated dianion in CuSMHD. Two quite distinct differences are noted in the bond lengths collected in Table 1. First and foremost, there has been a significant elongation, i.e. 0.08 Å, of the formally C1=S2 thione bond in SMHDH2 once this atom is complexed to Cu. Secondly, there has been a notable reduction, i.e. 0.05 Å, of the amine C1–N2 bond in SMHDH2, consistent with the formation of an imine bond in the complex. The reorganisation of electron density around the NCS_2 residue results in the contraction in the S–C–S angle with concomitant expansion in the angles involving the formally doubly bonded nitrogen atom, Table 1. In the crystal packing, molecules stack in columns aligned along the b-axis with no directional interactions between them.

The molecular structure of CuSBHD, Fig. 4a and Table 1, shows the same features as just discussed for CuSMHD, consistent with the notion that the nature of the S-bound substituent, methyl or benzyl, does not exert a significant difference upon the structure. This observation is highlighted in the overlay diagram shown in Fig. 4b. The seven-membered ring in CuSBHD has a half-chair conformation with the C4 atom lying 0.9970(19) Å above the plane defined by the Cu, N2, N3, C2, C3 and C5 atoms; r.m.s. = 0.2078 Å with maximum deviations 0.2432(7) Å for Cu and -0.3012(10) Å for N3. The aforementioned parameters indicate that this chelate ring is more distorted in CuSBHD cf. CuSMHD. With respect to the two five-membered chelate rings, the S1-containing ring is an envelope with the flap atom being the Cu atom which lies 0.7703(19) Å above the least-squares plane defined by the remaining four atoms (r.m.s. = 0.0004 Å), as is the S3-chelate ring with the Cu atom lying 0.423(2) Å above the plane of the four remaining atoms (r.m.s. = 0.0027 Å). In CuSBHD, the angle between the two five-membered chelate rings is 48.93(4)º, and the range of angles subtended at the Cu atom is 84.35(4)º for S3–Cu–N3 to 175.08(4)º for S1–Cu–N3, i.e. marginally broader than observed in CuSMHD, Table 1.

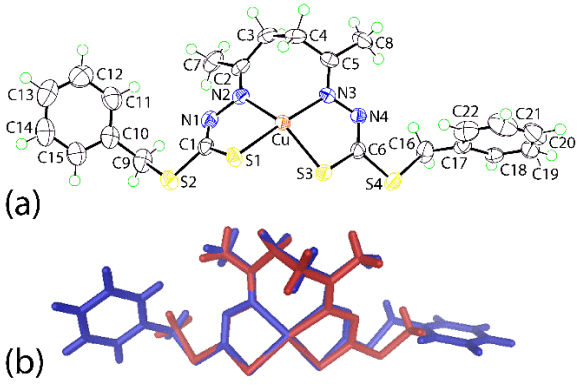

Fig. 4. (a) The molecular structure of CuSBHD, showing atom-labelling scheme, and (b) overlay diagram of CuSMHD (red image) and CuSBHD (blue). The complex molecules are overlapped so that the S1, Cu and S3 atoms are coincident.

The crystal packing of CuSBHD also resembles that of CuSMHD in that columns of molecules are evident, aligned along the a-axis. However, in CuSBHD molecules are linked by a combination of C–H…S and C–H…π (phenyl) interactions. Geometric parameters characterising the intermolecular interactions operating in the crystal structure of CuSBHD: C4–H4a...S4^{i} = 2.83 Å, C4...S4^{i} = 3.7647(16) Å, and angle at H4a = 158º for i: -x, -½+y, -½-z; C4–H4b...S3^{ii} = 2.84 Å, C4...S3^{ii} = 3.6946(19) Å, and angle at H4b = 145º for ii: -x, 1-y, -z; C18–H18...S4^{iii} = 2.86 Å, C18...S4^{iii} = 3.6811(17) Å, and angle at H18 = 145º for iii: x, 1½-y, -½+z; C3–H3a...Cg(C17–C22)^{i} = 2.89 Å, C3...Cg(C17–C22)^{i} = 3.6538(17) Å, and angle at H3a = 135º.

The observed four-coordinate structures described here for CuSBHD and CuSMHD, with the dianions in the iminothiolate form, is consistent with literature precedents [15, 16, 48-51].

Table 1

Selected geometric parameters (Å, º) for **SMHDH2**, **CuSMHD** and **CuSBHD**.

Compound	**SMHDH2**	**CuSMHD**	**CuSBHD**
Parameter			
Cu–S1	–	2.2480(4)	2.2458(4)
Cu–S3	–	2.2523(4)	2.2659(4)
Cu–N2	–	2.0555(12)	2.0704(13)
Cu–N3	–	1.9792(12)	1.9927(14)
C1–S1, S2	1.655(3), 1.763(3)	1.7373(14), 1.7579(14)	1.7354(16), 1.7573(17)
C6–S3, S4	–	1.7380(14), 1.7533(14)	1.7404(16), 1.7560(16)
N1–C1, N2–C2	1.339(3), 1.281(3)	1.2892(19), 1.2914(18)	1.286(2), 1.292(2)
N1–N2	1.391(3)	1.4182(16)	1.4181(18)
C5–N3, C6–N4	–	1.2872(18), 1.2887(18)	1.285(2), 1.286(2)
N3–N4	–	1.4073(16)	1.4019(18)
S1–Cu–S3	–	92.795(14)	91.655(15)
S1–Cu–N2	–	84.89(3)	85.26(4)
S1–Cu–N3	–	164.90(4)	175.08(4)
S3–Cu–N2	–	148.04(3)	148.89(4)
S3–Cu–N3	–	85.76(4)	84.35(4)
N2–Cu–N3	–	104.21(5)	99.65(5)
C1–N1–N2	119.2(2)	113.22(11)	113.38(12)
C2–N2–N1	117.0(2)	112.01(11)	112.92(13)
C5–N3–N4	–	115.20(11)	115.88(13)
C6–N4–N3	–	112.83(11)	112.70(12)
S1–C1–S2	123.83(16)	113.87(8)	111.63(9)
N1–C1–S1	122.7(2)	127.49(11)	128.34(13)
N1–C1–S2	113.51(18)	118.63(11)	120.01(12)
S3–C6–S4	–	113.94(8)	113.16(9)
N4–C6–S3	–	127.17(11)	126.59(12)
N4–C6–S4	–	118.89(10)	120.23(12)

Table 2

Crystallographic and refinement details for SBPY, SMHDH2, CuSMHD and CuSBHD.

Compound	**SBPY**	**SMHDH2**	**CuSMHD**	**CuSBHD**
Formula	$C_{14}H_{16}N_2S_2$	$C_{10}H_{18}N_4S_4$	$C_{10}H_{16}CuN_4S_4$	$C_{22}H_{24}CuN_4S_4$
Formula weight	276.41	322.52	384.05	536.23
Crystal colour/habit	Colourless plate	Yellow needle	Black prism	Black prism
Crystal dimensions/mm	0.04 x 0.20 x 0.21	0.03 x 0.06 x 0.24	0.04 x 0.12 x 0.18	0.11 x 0.22 x 0.28
Crystal system	monoclinic	triclinic	monoclinic	monoclinic
Space group	$P2_1/c$	$P\bar{1}$	$C2/c$	$P2_1/c$
a/Å	9.2991(4)	5.1646(5)	24.6441(8)	10.7937(1)
b/Å	15.9635(8)	7.2792(8)	7.9100(2)	18.8337(2)
c/Å	9.4848(5)	10.7840(12)	16.8972(6)	11.8412(2)
α/°	90	100.652(9)	90	90
β/°	96.155(1)	90.751(9)	111.167(4)	103.410(1)
γ/°	90	107.305(10)	90	90
V/Å^3	1399.87(12)	379.39(7)	3071.62(18)	2341.51(5)
Z	4	1	8	4
D_c/g cm^{-3}	1.312	1.412	1.661	1.521
F(000)	584	170	1576	1108
μ/mm^{-1}	0.364	5.662	1.956	1.308
Measured data	19199	4869	19072	58909
Radiation	MoKα	CuKα	MoKα	MoKα
θ range/°	2.5–27.5	4.2–71.6	2.6–27.5	2.2–27.5
Unique data	3207	1455	3490	5353
Observed data ($I \geq 2.0\sigma(I)$)	2722	1197	3291	4827
R, obs. data; all data	0.032; 0.041	0.046; 0.055	0.019, 0.021	0.028, 0.032
a, b in weighting scheme	0.030, 0.621	0.078, 0.048	0.032, 2.432	0.050, 1.156
R_w, obs. data; all data	0.071; 0.075	0.121; 0.130	0.054, 0.055	0.077, 0.080
Residual electron density peaks/e Å^3	0.30, -0.26	0.43, -0.28	0.37, -0.31	0.67, -0.47

2.3. Solution characterization of the complexes

The UV-Vis absorption spectra of the compounds for 25 μM and 1 mM solutions (inset) in DMSO are shown in Figure 5. Both complexes showed $\pi \rightarrow \pi^*$ and $n \rightarrow \pi^*$ intra-ligand transitions at *ca.* 272 nm, 295 nm and 338 nm and a *d-d* band at approximately 600 nm that can be attributed to Jahn-Teller distortion from square planar geometry [47]. Copper(II) complexes of thiosemicarbazone and dithiocarbazate ligands generally exhibit a S→Cu(II) charge-transfer band at ~400 nm. The presence of this LMCT band in the spectra of the metal complexes is strong evidence that the metal ion is coordinated to sulphur [43, 52].

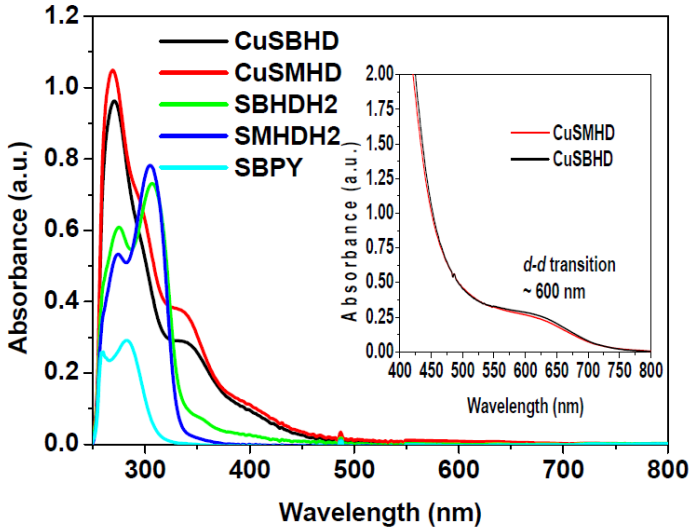

Fig. 5. UV-Vis spectra recorded at 25 μM in DMSO using a cell length of 1 cm. The insert shows the *d-d* band of the two complexes at concentration of 1 mM.

The stability of the ligands and their corresponding complexes at physiological pH are important prerequisites for the evaluation of their biological activity. The molar conductance readings for the complexes in DMSO were in the range 12-13 Ω^{-1} cm^2 mol^{-1}, indicating that there is essentially no dissociation in that solvent [53]. To more precisely evaluate their stability, reverse phase HPLC experiments have been performed. The ligands and their complexes were eluted on a C18-column with an increasing amount of CH_3CN in H_2O (from 5% to 100% of CH_3CN over 30 minutes), containing 0.1 % TFA to maintain pH. The compounds were detected using a UV lamp at 220 nm and 280 nm. The chromatograms of the pure ligands showed three peaks that could correspond to the hydrolyzed hydrazone, the expected ligand and the pyrrole byproduct whereas the complexes showed only the single peak of the copper complexes (see Supplementary Data). It is noteworthy that the hydrazone

bond stability is significantly increased upon metal-complexation under acidic conditions suggesting that complexation could be used as a means to protect the ligand from degradation that might occur in biological systems before free ligand could reach its target.

2.4. Electron Paramagnetic Resonance (EPR)

The EPR spectra recorded in DMF shown in Figure 6 are typical of Cu(II) complexes having axial symmetry and distorted square planar geometry with the unpaired electron mainly in the d_{x2} - d_{y2} orbital. The spectra also exhibit partially resolved superhyperfine features. The $g_{\|}$ values for all the complexes are similar to those previously reported for analogous Cu(II)N_2S_2 complexes [16, 25, 54]. Kivelson and Nieman [55, 56] suggested that $g_{\|}$ values higher than 2.3 are indicative of a predominantly ionic character for metal-ligand bonds, whereas $g_{\|}$ values smaller than 2.3 reveal metal-ligand bonds of predominantly covalent character, as is the case here (see Table 3). In addition, the relatively small $g_{\|}$ value ($g_{\|}$ ~2.20) suggests a strong nitrogen character in the singly occupied molecular orbital. EPR spectroscopy is sensitive to angular distortions at the Cu(II) centre, particularly those involving distortions from planar to tetrahedral geometry. As a general rule, distortion from planar towards tetrahedral geometry results in a decrease in $A_{\|}$ and an increase in $g_{\|}$ [52]. The empirical factor f (= $g_{\|}/A_{\|}$) [57, 58] is a measure of deviation from idealized geometry. Its value ranges between 105 and 135 cm for square planar complexes, depending on the nature of coordinated atoms, while, for tetrahedral structures, values from 160 to 242 cm suggest a moderate to considerable tetrahedral distortion. CuSBHD displays a slightly higher degree of tetrahedral distortion than CuSMHD in solution similar to their structures in solid. They are also slightly more distorted compared to some analogues, probably due to their extended carbon backbones [16, 25, 54]. Molecular orbital coefficients, α^2 (in-plane σ-bonding), were calculated using the equation below: [42, 59]

$$\alpha^2 = (A_{\|} / 0.036) + (g_{\|} - 2.0036) + 3 / 7\ (g_{\perp} - 2.0036) + 0.04$$

An α^2 value of 0.5 indicates complete covalent bonding, while 1.0 suggests complete ionic bonding. The observed value of 0.64 for the present complexes indicates that these copper complexes have some covalent character, as suggested above.

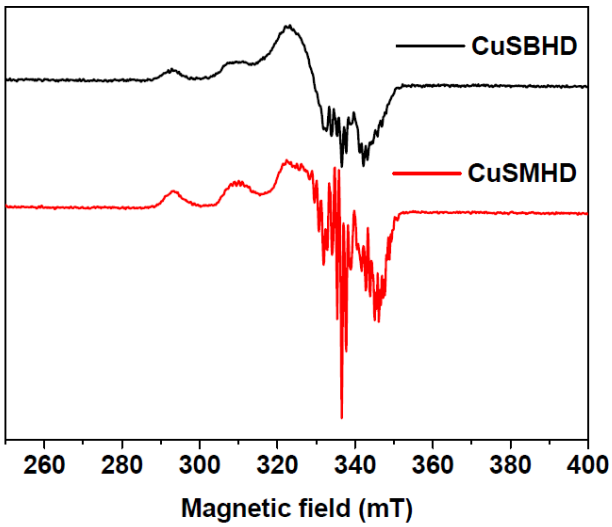

Fig. 6. EPR spectra of CuSBHD in black and CuSMHD in red recorded at a microwave frequency 9.50 GHz, power 0.25 mW, modulation amplitude 0.2 mT, modulation frequency 100 kHz, and time constant 164 ms, at 50 K. Samples were prepared in DMF (1 mM).

Table 3

EPR parameters measured from the spectra of the copper(II) complexes in DMF.

	$g_{\|}$	$g_{\perp}$	$A_{\|}$[a]	f[b]	α^2
CuSMHD	2.15	2.06	460 (153)	141	0.64
CuSBHD	2.16	2.06	451 (150)	143	0.64

[a] Unit in MHz, in bracket = $A_{\|}$ x 10^{-4} cm^{-1} [b] cm.

2.5. Electrochemistry

As redox properties have been linked to SOD and anticancer properties of metal complexes [60, 61], we describe herein the electrochemical properties of Cu(II) bis(dithio carbazate). Figure 7 shows the profile of the Cu(II) complexes obtained with SMHDH2 and SBHDH2 at scan rate 100 mV s^{-1}. Both complexes undergo an electrochemically irreversible one-electron reduction at E_{pc} = -0.328 and -0.285 V/(AgCl/Ag and Fc^{+}/Fc = 0.563 V), respectively, coupled with oxidation at E_{pa} = 0.069 and 0.129 V/(AgCl/Ag). These waves can be assigned to the irreversible oxidation/reduction of Cu(II)/Cu(I) [51]. The redox properties of the ligands were found to be innocent. The irreversible nature of the copper-centered redox waves contrasts with the quasi-reversible reduction previously reported for the CuATSM and CuAATSM analogues [49, 50]. The loss of reversibility observed in this work is most likely related to differences in the geometric rearrangement about the Cu(II)/Cu(I) ions in this

ligand system that possesses two carbons between the two hydrazone functions. The Cu(II)/Cu(I) redox potentials of CuSMHD and CuSBHD are also more positive than the previous examples. The ease of deformation seems to favour reduction. The difference in redox potential between CuSMHD and CuSBHD can be due to changes in inductive effects of the substituents. The increase in Cu redox potentials resulting from altering the terminal S-substituent (from methyl to benzyl) can be rationalized by the stronger electron-donating effect of the methyl group [62].

As mentioned above, the oxidation proceeding at higher positive potential has previously been assigned to the copper(III/II) redox couple. It is interesting to note the occurrence of an additional peak, which can be attributed to the reduction of a species produced by the second oxidation. However, the nature of this oxidized complex has not been determined.

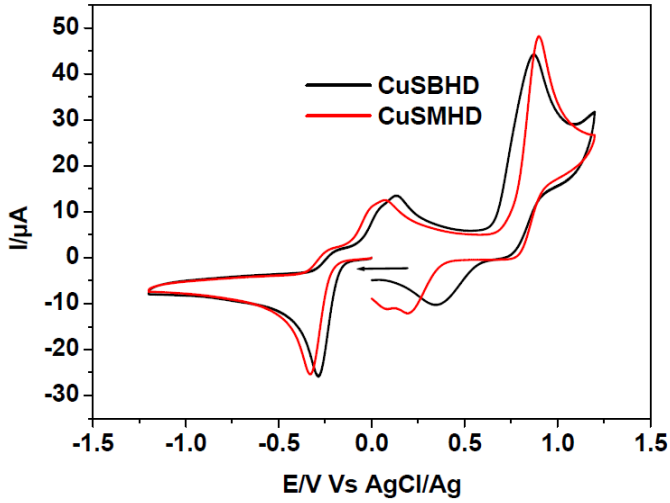

Fig. 7. Cyclic voltammograms of the Cu complexes at 1.7 mM in anhydrous deoxygenated DMF containing 0.1 M tetrabutylammonium hexafluorophosphate as the supporting electrolyte. Working electrode: glassy carbon; counter electrode: Pt wire; reference electrode: AgCl/Ag, scan rate: 100 mV/s. All sweeps were initiated in the direction of the arrow.

Table 4

Electrochemical data for CuSMHD and CuSBHD versus AgCl/Ag.

	Cu(II)/Cu(I)		Cu(III)/Cu(II)	
	E_{pc}/V	E_{pa}/V	E_{pc}/V	E_{pa}/V
CuSMHD	-0.328	0.069	0.195	0.899
CuSBHD	-0.285	0.129	0.357	0.870

3. Biological evaluation

3.1. Antibacterial activity

The free Schiff base ligands and their metal complexes were tested for their ability to inhibit the growth of ten strains of Gram-negative and Gram-positive bacteria (Table 5). The effects of a membrane permeabilizing agent and efflux pumps were investigated in an attempt to correlate the activity of the compounds with their penetration of the bacteria and the resistance mechanisms of the bacteria.

One of the limitations of this class of compounds is their poor solubility in aqueous solution particularly at high concentration to make stock solutions. The universal solvent DMSO has often been used in many studies to pre-dissolve the compounds for biological assays. However, it has been shown that DMSO solutions (1% to 10%) considerably affect the growth of fungi and cancerous cells, and, at 15%, DMSO effectively eliminates the growth of certain bacteria [63-65]. DMSO has also been reported to enhance permeability of the lipid membrane as well as to cause cell membranes to become less rigid facilitating membrane diffusion of exogenous species [66-69]. As DMSO is used in this work to encourage dissolution of the compounds and there is no rule of thumb on the amount of DMSO to be used for antibacterial assay, we feel the need to examine the influence of DMSO concentrations on the growth curve of the selected bacteria strains. The minimum inhibition concentration (MIC) values were determined in presence of DMSO at 0.5% and 5% (v:v) of DMSO. We found that the growth of bacteria strains *A. baumannii* and *P. aeroginosa* is inhibited by DMSO at a concentration of only 5% thus preventing determination of MIC under this condition. The growth of bacteria *E. coli* and *E. aerogenes* (see Supplementary Data) was also affected by the DMSO at 5%. Differences were observed between MIC values against the mutated strains *E. coli* AcrAB- and *E. aerogenes* 298 TolC- obtained in the presence of 0.5% or 5% DMSO for certain molecules, in particular, CuSMHD. Additional MIC values determined for CuSMHD using DMSO 50%, 30% and 20% (2.5%, 1.5% and 1% final v:v DMSO) were all higher than 128 µM while with 5% of DMSO, the MIC value was in the range of 1-2 and 0.5-1 µM against those two strains, respectively. Because of the effect of DMSO on bacterial growth, we are unable to confirm that the value truly reflects the specific antimicrobial activity of the compound alone. It could correspond to a synergetic effect involving the compound and DMSO. Since 0.5% DMSO has shown not to interfere with bacterial growth, the MIC values recorded using this concentration should indeed be

valid and are therefore used for discussion of the role of membrane permeabilizing agents and efflux pumps.

As it has been reported that low permeability of the outer membrane and the efficiency of efflux pumps [3, 4] are prime factors limiting intracellular activity of potential antimicrobial compounds, it is expected that the presence of a substance known to increase membrane permeability, such as polymyxin B nonapeptide (PMBN) [70], would act synergistically with the studied compounds to promote their antimicrobial efficiency by facilitating an increase in their uptake. The compounds were tested in the presence and absence of sub-inhibitory concentrations (1/5 of its direct MIC value) of PMBN. In the absence of PMBN none of the compounds except for SMHDH2 was active against the strains tested (MIC $\geq$ 64 µM). SMHDH2 showed moderate activity against *S. aureus.* However, up to 3-fold improvement in activity (MIC values) was observed for the organic compounds SMHDH2, SBHDH2 and SBDP in the presence of PMBN against both Gram-negative and Gram-positive bacteria. These results strongly suggest that the compounds apparent lack of activity was due to their inability to efficiently penetrate the bacteria membrane. Among the compounds, the Schiff base SMHDH2 showed a broad range of moderate activity against various strains with the most promising MIC values at or around 16 µM against *E. coli* AcrAB-, *A. baumannii*, *P. aeroginosa* and *S. aureus*, thus making it a potential antimicrobial agent in the presence of PMBN. It is known that the biological activity of dithiocarbazate compounds can be greatly modified by the presence of different substituents. For instance, inhibition of *E. coli* and *S. aureus* by the Schiff base prepared from 2-benzoylpyridine with S-methyldithiocarbazate (SMDTC) is highly effective whereas that of the S-benzyldithiocarbazate (SBDTC) analog shows no activity [71]. The better activity for SMDTC-derived SMHDH2 observed compared to SBDTC derivative is consistent with the previous report.

Table 5

Antibacterial activity of the tetradentate series.

Compound	Minimum Inhibitory Concentration (MIC) (μM)															
	Gram-														Gram+	
	E. coli				*E. aerogenes*				*A. baumannii*	*K. pneumoniae*		*P. aeruginosa*	*S. enterica*		*S. aureus*	
	AG100 WT		AG100A AcrAB-		EA289 AcrAB+		EA298 TolC-		ATCC 19606	ATCC 11296		PA01	SL696		SA1199	
% DMSO	0.5	5	0.5	5	0.5	5	0.5	5	0.5	0.5	5	0.5	0.5	5	0.5	5
SMHDH2	>128	>128	>128	>128	>128	128-64	>128-128	>128	64	128	64	128-64	>128	>128	32	64-32
+PMBN	32	32	16	16	>128-128	64	128	32	16	64	32-16	16-8	64	32	32-16	64-32
CuSMHD	>128	>128	>128	>128	>128	>128	>128	>128	>128	>128	>128	>128	>128	>128	>128	>128
+PMBN	>128	>128	>128	1-2	>128	>128	>128-128	0.5-1	>128	>128	>128	>128	>128	>128	>128	>128
SBHDH2	>128	128	>128	128	>128	128-64	>128-128	64	>128	>128	128	>128	>128	>128	>128	64-32
+PMBN	>128	64	128-32	32-16	>128-128	64	>128-64	16-4	128-64	128-64	32-16	64-32	>128	64	16	128
CuSBHD	>128	>128	>128	>128	>128	>128	>128	>128	>128	>128	>128	>128	>128	>128	>128	>128
+PMBN	>128	>128	>128	>128	>128	>128	>128	>128	>128	>128	>128	>128	>128	>128	>128	>128
SBPY	>64	>64	>64	>64	>64	>64	>64	>64	>128	>128	>128	>128	>128	>128	128	128-64
+PMBN	64	64	32	16	>64	64	32	4	>128-128	>128	64	>128-128	64	64-32	128-64	128
$Cu(Ac)_2$	>128	>128	>128	>128	>128	>128	>128	>128	>128	>128	>128	>128	>128	>128	>128	>128
+PMBN	>128	>128	>128	>128	>128	>128	>128	>128	>128	>128	>128	>128	>128	>128	>128	>128

Colour code: MIC values or average MIC values ≥ 64 μM = red, ≤10 μM = green, in between 64 μM and 10 μM = colourless. MIC values higher than 64 μM indicate poor activity.

The role of efflux pumps was investigated using pump-deleted strains of Gram-negative *E. coli and E. aerogenes*. Both SMHDH2 and SBPY seemed more active (16 µM and 32 µM, respectively) towards the isogenic derived strain, in which the efflux pump AcrAB genes are deleted as compared to wild-type *E. coli* (64 µM). No significant activity was observed for SMHDH2 in the absence likewise in presence of efflux pump for *E. aerogenes.* SBPY on the other hand showed differences in the MDR clinical isolate EA289 overexpressing the AcrAB efflux pump and on its efflux negative TolC- derivative EA298 with improvement in MIC from > 64 µM to 32 µM. These results confirmed that SBPY and SMHDH2 are recognized by the efflux pumps and expelled from the bacteria thus limiting their bioactivity. Both SMHDH2 and SBHDH2 showed activity towards Gram-positive *S. aureus.* Typically, antibacterial molecules are more active toward Gram-positive than Gram-negative bacteria [72, 73], as the additional outer membrane of the latter organisms impairs or slows down the drug uptake. It has often been reported in the literature that bioactivity of a ligand is enhanced by metal complexation [48, 57], but in our case, the formation of the copper complexes induces a loss of antibacterial potency of the compounds. Similar loss in activities were previously reported with palladium(II) and platinum(II) complexes with acetone Schiff bases [7]. This can be explained by a lower solubility of the metal complexes or by the lower stability of the hydrazone moiety in the case of the free ligands, as seen above. As mentioned before, depending on the pH, the ligands can be hydrolyzed in aqueous solution leading to several reactive products that can interfere with the bacteria constituents and be responsible for the toxicity. At this stage it is not possible to conclude but the positive effects of high DMSO concentration on the one hand, and of PMBN on the other, strongly suggest that improvements can be expected by increasing the solubility and bacteria penetration. Efforts are currently ongoing to significantly improve the aqueous solubility.

3.2. Cytotoxic assay

The cytotoxicity of the ligands and complexes was evaluated *in vitro* against two breast cancer cell lines MDA-MB-231 (human breast carcinoma cells not expressing nuclear estrogen receptors) and MCF-7 (human breast carcinoma cells expressing nuclear estrogen receptors). Measurement of the cytotoxicity was carried out using MTT assay [74] based on the metabolic reduction of tetrazolium salt to form water insoluble formazan crystals, with tamoxifen as standard. DMSO was used as negative control in the assay and the final content of DMSO for each compound tested was ≤ 0.5%. There was no perceptible precipitation of

the compounds. The concentrations required to inhibit the growth of cancer cells by 50% (IC_{50}) are shown in Table 6.

Table 6

Cytotoxic assay results.

	IC_{50} (μM)	
	MCF-7	MDA-MB-231
SMHDH2	138.90	9.61
SBHDH2	9.69	1.05
CuSMHD	2.60	2.34
CuSBHD	1.49	0.71
Tamoxifen	11.20	13.40

Both ligands displayed at least 9-fold better toxicity towards the MDA-MB-231 cell line that does not express estrogen nuclear receptors, indicating that ligand toxicity is not only mediated by these receptors. SBHDH2 exhibits a stronger toxicity, which could be related to its comparatively higher lipophilicity that may facilitate diffusion into cells [12]. Complexation of the Schiff base ligands with copper(II) has been found to produce synergistic effects on the antiproliferative activities of some parent ligands [75] and here the complexes showed a marked cytotoxicity with IC_{50} values < 5.0 μM towards both cell lines. Like the ligands, the complexes are also more active towards MDA-MB-231 cells, suggesting that their toxicity does not involve estrogen receptors. For both cell lines, the benzyl substituted complex CuSBHD showed slightly higher IC_{50} values. A clear structure-activity relationship cannot be deduced from the limited number of compounds tested, however, the stronger activity of CuSBHD could also be linked with its higher cellular uptake due to its increased lipophilicity as suggested above for the ligand. Alternatively, its higher redox potential could be a discriminating factor, since a higher redox potential means that Cu(II) reduction is easier, and consequently a higher content of Cu(I) could be generated. Cu(I) is prone to participate in Fenton-type reactions that produce reactive oxygen species (ROS), which can damage biomolecules within cells [61].

4. Conclusions

In conclusion, we have gained new insight into the structural, electrochemical and biological aspects of macroacyclic Cu(II) complexes derived from S-substituted dithiocarbazate. All the compounds exhibited good cytotoxicity towards breast cancer cells.

The poor antimicrobial activity can be related to their poor bacterial penetration and poor solubility which should be amenable to improvement. The fact that the anticancer activity Cu(II) complexes are more efficient than the ligands is interesting. By expanding the carbon backbone between the hydrazone moities, the compounds showed further distortion from square planar geometry in both solution and in the solid state and a positive shift in the Cu(II)/Cu(I) reduction potential. A higher reduction potential could be related to the promising bioactivity observed in this present work. Taking into consideration the serious side effects and the poor efficacy of clinical reference drugs, as well as the appearance of resistance during treatment, these complexes are potentially useful lead candidates for the development of new therapeutic agents to treat cancer and bacterial infections. In addition, we outlined in this paper the need to take into consideration the concentration of DMSO used to dissolve the compounds, since DMSO may act synergistically with the compounds tested. The lack of uptake of the compounds due to low permeability of the outer membrane and the efficiency of efflux pumps were also shown to be issues to be addressed in subsequent studies. With these considerations in mind, our group is attempting to improve antimicrobial and anticancer activities of compounds in this family by exploring the design and synthesis of a new generation of S-substituted dithiocarbazate derivatives and their metal complexes that will be more water-soluble, that may be better able to penetrate cell membranes and escape from the efflux pump.

5. Experimental

5.1. Materials-instrumentation-physical measurements

All chemicals and solvents were of analytical grade and were used as received. Chemicals: Potassium hydroxide (Merck), hydrazinium hydroxide (Merck), carbon disulfide (Sigma Aldrich), 2,5-hexanedione (Merck), and copper(II) acetate monohydrate (Analar). The IR spectra were recorded in the range of 550-4000 cm^{-1} on a Perkin-Elmer 100 series FT-IR spectrophotometer in ATR mode. Magnetic susceptibility was measured with a Sherwood MSB-AUTO at room temperature. All susceptibilities were corrected for the diamagnetic contribution using Pascal's constant. Microanalyses were carried out using either a Leco CHNS-932 analyzer or performed at the CNRS (Gif-sur-Yvette and Vernaison, France). The molar conductance of a 10^{-3} M solution of each metal complex in DMSO was measured at 29°C using a Jenway 4310 conductivity meter and a dip-type cell with platinized electrode. The UV-Vis spectra were recorded on a Cary 300 bio spectrophotometer (200-800

nm) or Perkin Elmer Lambda 45 with a 1 cm optical path quartz cuvette. ^{1}H NMR and ^{13}C NMR spectra were recorded with Bruker DRX300 spectrometers. The chemical shifts (δ/ppm) were calibrated relative to residual solvent signals**.** Electrospray-ionization mass spectra (ESI-MS) were recorded with a Finnigan Mat 95S in the BE configuration at low resolution. Electron paramagnetic resonance (EPR) spectra were recorded on an X-band Bruker Elexsys 500 spectrometer equipped with a continuous flow helium cryostat (Oxford Instruments) and a temperature control system. The field modulation frequency was 100 kHz. The spectra were all recorded under nonsaturating conditions. Cyclic voltammetry (CV) measurements were recorded under argon using a 620C electrochemical analyzer (CH Instruments, Inc). The working electrode was a glassy carbon disk; a Pt wire was used as counter electrode and the reference electrode was an AgCl/Ag electrode. Immediately before the measurement of each voltammogram, the working electrode was carefully polished with alumina suspensions (1, 0.3 and 0.05 μm, successively), sonicated in an ethanol bath and then washed carefully with ethanol. The solutions were made up with 100 μL solutions of the complexes (0.01 M) in anhydrous deoxygenated DMF with 0.5 mL of tetrabutylammonium hexafluorophosphate (0.1 M) as the supporting electrolyte (total volume is 0.6 mL). Ferrocene was used as an internal reference for which the ferrocinium/ferrocene one-electron redox process occurs at $E_{1/2}$ = 0.51 V (DMF) vs AgCl/Ag with scan rate = 0.1 V/s. RP-HPLC analysis was carried out using Waters HPLC system connected to Breeze software that consisted of combination of a dual wavelength UV-Vis absorbance detector (Waters 2487) and a binary pump (Waters 1525) equipped with an analytical cell for reaction monitoring or purity checking. The analytical measurements were performed using an ACE C18 column (250 × 4.5mm) packed with spherical 5 μm particles of 300 Å pore size. Experiments were carried out at a flow rate of 1 mL min^{-1} at room temperature. Injection volume was 50 μL. Sample concentration was approximately 1 mg mL^{-1}.

5.2. Preparation of ligands and metal complexes

5.2.1 Synthesis of SBHDH2

The title compound was synthesized with some modification of the method described by Ali *et al.* [35]. 2,5-hexandione (0.587 mL, 0.005 mol, 1 equiv.) was added to a hot solution of S-benzyldithiocarbazate (1.983 g, 0.01 mol, 2 equiv.) in absolute ethanol (150 mL) and the mixture was further heated for 5 min. A white precipitate was formed and was immediately filtered off, washed with cold ethanol and dried *in vacuo* over silica gel to yield the expected Schiff base (0.997 g, Yield = 42%). Elemental analysis for $C_{22}H_{26}N_4S_4$: Calcd.

C 55.66, H 5.52, N 11.80; Found C 54.79, H 5.59, N 11.75. ^{1}H NMR (300 MHz, DMSO-d6) δ 12.18 (s, 2H), 7.39 -7.20 (m, 10H), 4.40 (s, 4H), 1.96 (s, 6H). ^{13}C NMR (75 MHz, DMSO-d6) δ 197.16, 158.26, 137.15, 129.15, 128.41, 127.05, 37.56, 34.05, 17.74. IR: ν (cm^{-1}) = 3147 (m, b), 1640 (w), 1054 (s), 981 (m), 828 (m). UV-Vis in DMSO: λ_{max} nm (log ε in $L\,mol^{-1}\,cm^{-1}$) = 276 (4.32), 308 (4.41), ≈360 (3.32, sh). RP-HPLC: R_T (min) = 15.3, 18.3, 22.4. Molar conductivity: Λ ($ohm^{-1}cm^2mol^{-1}$) = 6.86.

5.2.2 Synthesis of SMHDH2

S-methyldithiocarbazate, SMDTC (1.222 g, 0.01 mol, 2 equiv.) was dissolved in hot ethanol (150 mL) and 2,5-hexandione (0.587 mL, 0.005 mol, 1 equiv.) was added to this solution. The mixture was heated while being stirred to reduce the volume to half. The mixture was kept at 4°C overnight and white precipitate was formed. The product was filtered off, washed with cold ethanol and dried *in vacuo* over silica gel to afford 1.129 g of SMHDH2 (Yield = 70%). The compound was further recrystallised from methanol and crystals suitable for X-ray diffraction analysis were obtained from the same solvent. Elemental analysis for $C_{10}H_{18}N_4S_4$: Calcd. C 37.24, H 5.63, N 17.37; Found C 37.86, H 4.87, N 17.84. ^{1}H NMR (300 MHz, DMSO-d6) δ 12.13 (s, 2H), 2.57 (s, 4H), 2.43 (s, 6H), 2.00 (s, 6H). ^{13}C NMR (75 MHz, DMSO-d6) δ 198.95, 157.63, 33.97, 17.77, 16.94. IR: ν (cm^{-1}) = 3111 (m, b), 1628 (m), 1046 (s), 988 (m), 827 (m). UV-Vis in DMSO: λ_{max} nm (log ε in $L\,mol^{-1}\,cm^{-1}$) = 276 (4.25), 305 (4.37), ≈360 (2.75, sh). RP-HPLC: R_T (min) = 6.4, 11.1, 18.7. Molar conductivity: Λ ($ohm^{-1}cm^2mol^{-1}$) = 3.58

5.2.3. Synthesis of CuSBHD

The copper complex was prepared by adding copper (II) acetate monohydrate (0.020 g, 0.0001 mol, 1 equiv.) in acetonitrile (20 mL) to a solution of SBHDH2 (0.047 g, 0.0001 mol, 1 equiv.) in acetonitrile (150 mL) at room temperature. The solution was stirred for an hour and then concentrated to reduce volume before being placed at 4°C overnight. The product was filtered off and recrystallised from acetonitrile to yield 0.039 g (Yield = 73%). Black crystals of diffraction quality were crystallized from acetonitrile after several days through slow evaporation at 4°C. Elemental analysis for $C_{22}H_{25}CuN_4S_4$: Calcd. C 49.27, H 4.51, N 11.85; Found C 49.40, H 4.63, N 10.46. ESI-MS: *m*/*z* = $[M+H]^+$ Calcd. 536.04, Found 536.02; $[M+Na]^+$ Calcd. 558.02, Found 558.01; $[M+K]^+$ Calcd. 573.99, Found 573.98; $[2M+3H]^+$ Calcd. 1073.08, Found 1073.04. IR: ν (cm^{-1}) = 1629 (m), 1606 (w), 992 (s), 955

(s), 857 (m). UV-Vis in DMSO: λ_{max} nm (log ε in L mol^{-1} cm^{-1}) = 275 (4.37), ≈294 (4.26, sh), ≈340 (4.01, sh), ≈400 (3.55, sh), ≈600 (2.45, sh). RP-HPLC: R_T (min) = 28.5. Magnetic moment: μ (B.M.) = 1.48. Molar conductivity: Λ (ohm^{-1}cm^{2}mol^{-1}) = 13.01.

5.2.4. Synthesis of CuSMHD

The copper complex was prepared by adding copper (II) acetate monohydrate (0.200 g, 0.001 mol, 1 equiv.) in methanol (20 mL) to a hot solution of the above SMHDH2 (0.322 g, 0.001 mol, 1 equiv.) in methanol (100 mL). The reaction was heated until the volume reduced to half and then placed at 4°C overnight. The product, which formed, was filtered off and recrystallised from acetonitrile to afford 0.296 g of CuSMHD (Yield = 77%). Black crystals of diffraction quality crystallized from acetonitrile after several weeks through slow evaporation at room temperature. Elemental analysis for: $C_{10}H_{17}CuN_4S_4$: Calcd. C 31.27, H 4.20, N 14.59; Found C 31.35, H 4.24, N 14.64. ESI-MS: *m*/*z* = $[M + H]^+$ Calcd. 383.97, Found 383.96; $[M+Na]^+$ Calcd. 405.96, Found 405.94; $[M+K]^+$ Calcd. 421.93, Found 421.92. IR: ν (cm^{-1}) = 1628 (m), 1611(w), 1000 (s), 964 (s), 821 (m). UV-Vis in DMSO: λ_{max} nm (log ε in L mol^{-1} cm^{-1}) = 273 (4.34), ≈294 (4.24, sh), ≈340 (3.99, sh), ≈400 (3.49, sh) ≈600 (2.43, sh). RP-HPLC: R_T (min) = 23.3. Magnetic moment: μ (B.M.) = 1.66. Molar conductivity: Λ (ohm^{-1}cm^{2}mol^{-1}) = 12.80.

5.2.5. Synthesis of SBPY

SBPY was a side product from the initial attempt to synthesize SBHDH2. Prolonged heating and purification *via* column chromatography caused the desired compound to undergo cyclization forming a pyrrole. Single crystals of diffraction quality were obtained from DMSO and analyzed by single crystal X-ray diffraction. ESI-MS: *m*/*z* = $[M + H]^+$ Calcd. 277.08, Found 277.08; $[M + Na]^+$ Calcd. 299.07, Found 299.06. ^{1}H NMR (300 MHz, DMSO-d6): δ (ppm) = 12.29 (s, 1H), 7.45 – 7.20 (m, 5H), 5.69 (s, 2H), 4.45 (s, 2H), 2.00 (s, 6H). ^{13}C NMR (75 MHz, DMSO-d6): δ (ppm) = 204.09, 136.30, 129.02, 128.55, 127.43, 126.50, 104.34, 38.17, 10.99. IR: ν (cm^{-1}) = 3264 (m), 2917 (w), 1055 (s), 972 (w), 828 (w). UV-Vis in DMSO: λ_{max} nm (log ε in L mol^{-1} cm^{-1}) = 282 (4.02). RP-HPLC: R_T (min) = 22.3.

5.3. Biological studies

5.3.1. In vitro cytotoxicity testing

The cell lines used for testing included MCF-7 (human breast cancer cells possessing nuclear esstrogen receptor) and MDA-MB-231 (human breast cancer cells without nuclear estrogen receptor) were obtained from the National Cancer Institute, U.S.A. Both cell lines were cultured in RPMI-1640 / DMEM (High glucose) (Sigma) medium supplemented with 10% fetal calf serum. The cells were plated into 96-well plates at cell density 6000 cells/well and incubated for 24 hours. After 24 hours, the media (5% serum) were discarded and cells rinsed with PBS solution. 200 µL of a series of concentration (50.0, 25.0, 10.0, 5.0, 1.0 and 0.5 µM) for each samples prepared were added to each well. The 96-well plate was incubated for another 72 hours. After 72 hours, 96-wells plate was removed from incubator. Cytotoxicity was determined using the microtitration of 3-(4,5-dimethylthiazol-2-yl)-2,5-diphenyltetrazolium bromide (MTT) assay (Sigma, USA) as reported by Mosmann [74]. 20µL of MTT solution (5 mg/mL) was added to each well. The plate was wrapped with aluminium foil and incubated for 4 hours. After 4 hours, 200 µL of sample containing MTT solution was discarded from the well. 200 µL of DMSO was added to each well to dissolve the formazan crystals formed. The effect of the compound on cell lines viability was measured on an automated spectrophotometric plate reader (model MRX II microplate Elisa reader) at a test wavelength of 570 nm. Cytotoxicity was expressed as IC_{50}, i.e. the concentration that reduced the absorbance of treated cells by 50% with reference to the control (untreated cells). The IC_{50} were determined from the plotted absorbance data for the dose-response curves. Controls that contained only cells were included for each sample. Tamoxifen was used as the cytotoxic standard.

5.3.2. Antimicrobial testing

5.3.2.1. Bacterial strains, culture media and chemicals

The bacteria used in this study are listed in Table 7. The microorganisms studied included reference (from the American Type Culture Collection) and clinical (Laboratory collection) strains of Gram-negative bacteria *Escherichia coli, Enterobacter aerogenes, Acinetobacter baumannii, Klebsiella pneumoniae, Pseudomonas aeruginosa and Salmonella enterica* serotype Typhimurium as well as Gram-positive strain *Staphylococcus aureus.* EA289 is an *Enterobacter aerogenes* KAN^S (susceptible to kanamycin, MDR isolate that exhibits active efflux of norfloxacin and AcrAB-TolC pump overproduction), EA298 constructed from EA289 is deleted of TolC [76]. AG100 is an *E. coli* Wild Type (WT) and AG100A is its KAN^R (resistant to kanamycin) derivative, deleted of AcrAB and

hypersensitive to chloramphenicol, tetracycline, ampicillin and nalidixic acid [77]. Strains were grown at 37°C on Mueller-Hinton medium 24 h prior to any assay. Mueller-Hinton broth (MHB) was used for the susceptibility test. Chemicals polymyxin B nonapeptide (PMBN) was obtained from Sigma-Aldrich and the culture medium was purchased from Becton Dickinson.

Table 7: Bacteria strains.

Bacteria strains	**Features**	**References**
Escherichia coli		
AG100	Wild-type *E. coli* K-12	[77]
AG100A	AG100 ΔAcrAB::KAN^R	[77]
Enterobacter aerogenes		
EA289	KAN sensitive derivative of EA27	[76]
EA294	EA289 AcrA::KAN^R	[76]
EA298	EA 289 TolC::KAN^R	[76]
Acinetobacter baumannii		
ATCC19606	Reference strain	-
Klebsiella pneumoniae		
ATCC12296	Reference strain	-
Pseudomonas aeruginosa		
PA 01	Reference strain	-
***Salmonella enterica* serotype Typhimurium**		
SL696	Wild-type, metA22, trpB2, strAi20	[78]
Staphylococcus aureus		
SA1199	Wild-type clinical, methicillin-susceptible	[79]

KAN^R, resistance to kanamycin

5.3.2.2. Determination of bacterial susceptibility

The respective minimum inhibitory concentrations (MIC) of the samples against targeted bacteria were determined using the microdilution method (CLSI) [80]. Susceptibilities were determined in 96-well microplates with an inoculum of 2×10^5 cfu in 200 µL of MHB containing two-fold serial dilutions of samples. MICs were determined in the presence of 5% or 0.5% of DMSO. In the first case, a 20× concentration range of each compound was prepared in DMSO 100%. In the second case, a 200× concentration range of each compound was prepared in DMSO 100% and then diluted with H_2O to obtain a 20× concentration range in DMSO 10%. Then 10 µl of these ranges were added to 190 µl of inoculum reducing the DMSO concentration to 0.5%. The MICs of samples were determined after 18 h incubation at 37°C, following addition (50 µl) of 0.2 mg/mL iodonitrotetrazolium (INT) and incubation at 37°C for 30 minutes. MIC is defined as the lowest sample concentration that prevented the color change of the medium and exhibited complete inhibition of microbial growth. The sample dilution range was from 0-128 µM. Samples were tested alone or in the presence of PMBN at 51.2 mg/L final concentration (1/5 of its direct MIC). All assays were performed in duplicate or triplicate.

5.4. X-ray crystallography

X-ray diffraction measurements for SBPY were performed at 100 K on a Bruker Kappa X8 APEXII CD diffractometer with graphite monochromatised MoKα radiation (λ = 0.71073 Å). Correction for absorption was based on multi-scans [81]. Intensity data for SMHDH2, CuSMHD and CuSBHD were measured at 150 K on an Oxford Diffraction Gemini CCD diffractometer employing either CuKα (SMHDH2), λ = 1.54184 Å, or MoKα radiation (CuSMHD and CuSBHD). Again, the corrections for absorption were based on multi-scans [82]. The structures were solved by direct methods and refined (anisotropic displacement parameters, H atoms in the riding model approximation and a weighting scheme of the form $w = 1/[\sigma^2(F_o^2) + aP^2 + bP]$ where $P = (F_o^2 + 2F_c^2)/3)$ F^2 using SHELX programs [83] through the WinGX interface [84]. Crystal data and refinement details are collated in Table 2. The molecular structures shown in Figs 1-4 were drawn with 70% displacement ellipsoids using ORTEP-3 for Windows [84]. The overlay diagram, Fig. 4b, was drawn with QMol [85] and the crystal packing diagrams with DIAMOND [86].

Acknowledgements

Support for the project came from Universiti Putra Malaysia (UPM), the Ministry of Higher Education (Malaysia), French ANR Blanc 2010, METABACT grant and the French Infrastructure for Integrated Structural Biology (FRISBI) ANR-10-INSB-05-01. M. L. Low is grateful for the award of an Erasmus Mundus: Maheva Scholarship and a UPM Graduate Research Fellowship (GRF).

List of abbreviations

A. baumannii	*Acinetobacter baumannii*
CV	Cyclic voltammetry
DMEM	Dulbecco's modified Eagle's medium
DMF	Dimethylformamide
DMSO	Dimethyl sulfoxide
DMSO-d6	Deuterated dimethyl sulfoxide
E. aerogenes	*Enterobacter aerogenes*
E. coli	*Escherichia coli*
EPR	Electron paramagnetic resonance
ESI-MS	Electrospray ionization-mass spectra
FT-IR	Fourier transform-infrared spectroscopy
INT	Iodonitrotetrazolium
KAN^R	Resistance to kanamycin
KAN^S	Sensitive to kanamycin
K. pneumonia	*Klebsiella pneumonia*
LMCT	Ligand-to-metal charge-transfer
MCF-7	Human breast carcinoma cells expressing nuclear estrogen receptors
MDA-MB-231	Human breast carcinoma cells not expressing nuclear estrogen receptors
MDR	Multidrug resistance
MHB	Mueller-Hinton broth
MIC	Minimum inhibitory concentration
MTT	3-(4,5-dimethylthiazol-2-yl)-2,5-diphenyltetrazolium bromide
NMR	Nuclear magnetic resonance
ORTEP	Oak Ridge thermal ellipsoid plot
PBS	Phosphate buffered saline
PMBN	Polymyxin B nonapeptide
P. aeruginosa	*Pseudomonas aeruginosa*
ROS	Reactive oxygen species
RP-HPLC	Reversed phase-high performance liquid chromatography
r. t.	Room temperature
S. enterica	*Salmonella enterica*
SBDTC	S-benzyldithiocarbazate

SMDTC	S-methyldithiocarbazate
SOD	Superoxide dismutase
S. aureus	*Staphylococcus aureus*
UV-Vis	Ultraviolet-visible
WT	Wild type

Appendix A. Supplementary data

Supplementary data related to this article can be found at X.

The crystallographic data for the structural analysis of the compounds have been deposited with the Cambridge Crystallographic Data Centre, CCDC No. for SBPY is 1057065, SMHDH2 is 1057066, CuSMHD is 1057067 and for CuSBHD is 1057068. A copy of this information may be obtained free of charge from the Director, CCDC, 12 Union Road, Cambridge CB2 1EZ, UK (Tel.: +44 (0) 1223 762911; E-mail: deposit@ccdc.cam.ac.uk).

References:

[1] A. Coates, Y. Hu, R. Bax, C. Page, Nat. Rev. Drug Discov. 1 (2002) 895-910.

[2] G. Taubes, Science 321 (2008) 321, 356-361.

[3] J.-M. Pagès, L. Amaral, Biochim. Biophys. Acta - Proteins Proteom. 1794 (2009) 826-833.

[4] H. Nikaido, J.-M. Pagès, FEMS Microbiol. Rev. 36 (2012) 340-363.

[5] J. Ma, A. Jemal, in *Breast Cancer Metastasis and Drug Resistance,* Springer New York (2013) pp. 1-18.

[6] G. Yang, S. Nowsheen, K. Aziz, A. G. Georgakilas, Pharmacol. Ther. 139 (2013) 392-404.

[7] M. A. Ali, A. H. Mirza, R. J. Butcher, M. T. H. Tarafder, T. B. Keat, A. M. Ali, J. Inorg. Biochem. 92 (2002) 141-148.

[8] A. B. Beshir, S. K. Guchhait, J. A. Gascón, G. Fenteany, Bioorg. Med. Chem. Lett. 18 (2008) 498-504.

[9] M. L. Low, L. Maigre, P. Dorlet, R. Guillot, J.-M. Pagès, K. A. Crouse, C. Policar, N. Delsuc, Bioconjugate Chem. 25 (2014) 2269-2284.

[10] M. R. Maurya, S. Khurana, A. Azam, W. Zhang, D. Rehder, Eur. J. Inorg. Chem. 2003 (2003) 1966-1973.

[11] P. I. D. S. Maia, A. G. D. A. Fernandes, J. J. N. Silva, A. D. Andricopulo, S. S. Lemos, E. S. Lang, U. Abram, V. M. Deflon, J. Inorg. Biochem. 104 (2010) 1276-1282.

[12] F. R. Pavan, P. I. D. S. Maia, S. R. A. Leite, V. M. Deflon, A. A. Batista, D. N. Sato, S. G. Franzblau, C. Q. F. Leite, Eur. J. Med. Chem. 45 (2010) 1898-1905.

[13] T. B. S. A. Ravoof, K. A. Crouse, M. I. M. Tahir, F. N. F. How, R. Rosli, D. J. Watkins, Transit. Metal Chem. 35 (2010) 871-876.

[14] F. N. F. How, K. A. Crouse, M. I. M. Tahir, M. T. H. Tarafder, A. R. Cowley, Polyhedron 27 (2008) 3325-3329.

[15] M. A. F. A. Manan, M. I. M. Tahir, K. A. Crouse, R. Rosli, F. N. F. How, D. J. Watkin, J. Chem. Crystallogr. 41 (2011) 1866-1871.

[16] J. P. Jasinski, J. R. Bianchani, J. Cueva, F. A. El-Saied, A. A. El-Asmy, D. X. West, Z. Anorg. Allg. Chem. 629 (2003) 202-206.

[17] M. A. Ali, S. E. Livingstone, Coord. Chem. Rev. 13 (1974) 101-132.

[18] M. T. H. Tarafder, A. M. Ali, Y. W. Wong, S. H. Wong, K. A. Crouse, Synth. React. Inorg. Met.-Org. Chem. 31 (2001) 115-125.

[19] M. L. Low, G. Paulus, P. Dorlet, R. Guillot, R. Rosli, N. Delsuc, K. A. Crouse, C. Policar, Biometals, 28 (2015) 553-566

[20] P.A.Vigato, S. Tamburini, Coord. Chem. Rev. 248 (2004) 1717-2128.

[21] J. P. Holland, P. J. Barnard, S. R. Bayly, H. M. Betts, G. C. Churchill, J. R. Dilworth, R. Edge, J. C. Green, R. Hueting, Eur. J. Inorg. Chem. 2008 (2008) 1985-1993.

[22] M. Gennari, J. Pécaut, M. N. Collomb, C. Duboc, Dalton Trans. 41 (2012) 3130-3133.

[23] B. M. Paterson, P. S. Donnelly, Chem. Soc. Rev. 40 (2011)3005-3018; P. S. Donnelly, Dalton Trans. 40 (2011) 999-1010.

[24] D. B. Rorabacher, Chem. Rev. 104 (2004) 651-698; M. G. B. Drew, C. J. Harding, V. McKee, G. G. Morgan, J. Nelson, J. Chem. Soc., Chem. Commun. (1995) 1035-1038; S. Durot, C. Policar, F. Cisnetti, F. Lambert, J.-P. Renault, G. Pelosi, G. Blain, H. Korri-Youssoufi, J.-P. Mahy, Eur. J. Inorg. Chem. 2005 (2005) 3513-3523.

[25] A. Díaz, R. Pogni, R. Cao, R. Basosi, Inorg. Chim. Acta 275-276 (1998) 552-556.

[26] A. Díaz, R. Cao, A. Fragoso, I. Sánchez, Inorg. Chem. Commun. 2 (1999) 361-363.

[27] Q.-X. Li, H.-A. Tang, Y.-Z. Li, M. Wang, L.-F. Wang, C.-G. Xia, J. Inorg. Biochem. 78 (2000) 167-174.

[28] Z. Afrasiabi, E. Sinn, S. Padhye, S. Dutta, S. Padhye, C. Newton, C. E. Anson, A. K. Powell, J. Inorg. Biochem. 95 (2003) 306-314.

[29] T. Ngarivhume, A. Díaz, R. Cao, M. Ortiz, I. Sánchez, Synth. React. Inorg. Met.-Org. Nano-Met Chem 35 (2005) 795-800.

[30] M. A. Ali, C. M. Haroon, M. Nazimuddin, S. M. M. U. H. Majumder, M. T. H. Tarafder, M. A. Khair, Transit. Metal Chem. 17 (1992) 133-136.

[31] X. H. Zhu, S. H. Liu, Y. J. Liu, J. Ma, C. Y. Duan, X. Z. You, Y. P. Tian, F. X. Xie, S. S. Ni, Polyhedron 18 (1998) 181-185.

[32] M. A. Ali, P. V. Bernhardt, M. A. H. Brax, J. England, A. J. Farlow, G. R. Hanson, L. L. Yeng, A. H. Mirza, K. Wieghardt, Inorg. Chem. 52 (2013) 1650-1657.

[33] M. H. E. Chan, K. A. Crouse, M. I. M. Tahir, R. Rosli, N. Umar-Tsafe, A. R. Cowley, Polyhedron 17 (2008) 1141-1149.

[34] K. B. Chew, M. T. H. Tarafder, K. A. Crouse, A. M. Ali, B. M. Yamin, H. K. Fun, Polyhedron 23 (2004) 1385-1392.

[35] M.A. Ali, S.M.G. Hossain, S.M.M.H. Majumder, M.N. Uddin, M.T.H. Tarafder, Polyhedron 6 (1987) 1653-1656.

[36] R. N. Patel, K. K. Shukla, A. Singh, M. Choudhary, D. K. Patel, J. Niclós-Gutiérrez, D. Choquesillo-Lazarte, Transit. Metal Chem. 34 (2009) 239-245.

[37] A. T. Chaviara, P. J. Cox, K. H. Repana, A. A. Pantazaki, K. T. Papazisis, A. H. Kortsaris, D. A. Kyriakidis, G. S. Nikolov, C. A. Bolos, J. Inorg. Biochem. 99 (2005) 467-476.

[38] B. Jeragh, A. A. El-Asmy, Spectrochim. Acta A: Mol. Biomol. Spectrosc. 130 (2014) 546-552.

[39] B. Jeragh, A. A. El-Asmy, Spectrochim. Acta A: Mol. Biomol. Spectrosc. 129 (2014) 307-313.

874 [40] K. Liu, H. Lu, L. Hou, Z. Qi, C. Teixeira, F. Barbault, B. T. Fan, S. Liu, S. Jiang, L. Xie, J. Med. Chem. 51
875 (2008) 7843-7854.
876 [41] A. Fürstner, Angew. Chem. Int. Ed. 42 (2003) 3582-3603.
877 [42] P. F. Rapheal, E. Manoj, M. R. Prathapachandra Kurup, Polyhedron 26 (2007) 818-828.
878 [43] K. A. Crouse, K.-B. Chew, M. T. H. Tarafder, A. Kasbollah, A. M. Ali, B. M. Yamin, H. K. Fun,
879 Polyhedron 23 (2004) 161-168.
880 [44] M. A. Ali, M. T. H. Tarafdar, J. Inorg. Nucl. Chem. 39 (1977) 1785-1791.
881 [45] S. Belaid, A. Landreau, S. Djebbar, O. Benali-Baitich, G. Bouet, J.-P. Bouchara, J. Inorg. Biochem. 102
882 (2008) 63-69.
883 [46] M. Kato, H. B. Jonassen, J. C. Fanning, Chem. Rev. 64 (1964) 99-128.
884 [47] M. S. Nair, R.S. Joseyphus, Spectrochim. Acta A: Mol. Biomol. Spectrosc. 70 (2008) 749-753.
885 [48] A. K. Nandi, S. Chaudhuri, S. K. Mazumdar, S. Ghosh, Inorg. Chim. Acta 92 (1984) 235-240.
886 [49] P. J. Blower, T. C. Castle, A. R. Cowley, J. R. Dilworth, P. S. Donnelly, E. Labisbal, F. E. Sowrey, S. J.
887 Teat, M. J. Went, Dalton Trans. (2003) 4416-4425.
888 [50] A. R. Cowley, J. R. Dilworth, P. S. Donnelly, A. D. Gee, J. M. Heslop, Dalton Trans. (2004) 2404-2412.
889 [51] B. M. Paterson, J. A. Karas, D. B. Scanlon, J. M. White, P. S. Donnelly, Inorg. Chem. 49 (2010) 1884-
890 1893.
891 [52] M. A. Ali, A. H. Mirza, R. J. Fereday, R. J. Butcher, J. M. Fuller, S. C. Drew, L. R. Gahan, G. R. Hanson,
892 B. Moubaraki, K. S. Murray, Inorg. Chim. Acta 358 (2005) 3937-3948.
893 [53] M. T. Tarafder, M. Ali, D. J. Wee, K. Azahari, S. Silong, K. Crouse, Transit. Metal Chem. 25 (2000) 456-
894 460.
895 [54] R. Hueting, M. Christlieb, J. R. Dilworth, E. G. Garayoa, V. Gouverneur, M. W. Jones, V. Maes, R.
896 Schibli, X. Sun, D. A. Tourwe, Dalton Trans. 39 (2010) 3620-3632.
897 [55] R. C. Chikate, A. R. Belapure, S. B. Padhye, D. X. West, Polyhedron 24 (2005) 889-899.
898 [56] D. Kivelson, R. Neiman, J. Chem. Phys. 35 (1961) 149-155.
899 [57] J. Joseph, K. Nagashri, G. B. Janaki, Eur. J. Med. Chem. 49 (2012) 151-163.
900 [58] P. Murali Krishna, K. Hussain Reddy, J. Pandey, D. Siddavattam, Transit. Metal Chem. 33 (2008) 661-668.
901 [59] S. Chandra, X. Sangeetika, Spectrochim. Acta A: Mol. Biomol. Spectrosc. 60 (2004) 147-157.
902 [60] Z. Duracková, M. A. Mendiola, M. T. Sevilla, A. Valent, Bioelectrochem. Bioenerg. 48 (1999) 109-116.
903 [61] P. J. Jansson, P. C. Sharpe, P. V. Bernhardt, D. R. Richardson, J. Med. Chem. 53 (2012) 5759-5769.
904 [62] M. T. Basha, J. D. Chartres, N. Pantarat, M. Akbar Ali, A. H. Mirza, D. S. Kalinowski, D. R. Richardson,
905 P. V. Bernhardt, Dalton Trans. 41 (2012) 6536-6548.
906 [63] N. S. Ng, P. Leverett, D. E. Hibbs, Q. Yang, J. C. Bulanadi, M. Jie Wu, J. R. Aldrich-Wright, Dalton Trans.
907 42 (2012) 3196-3209.
908 [64] R. Notman, M. Noro, B. O'Malley, J. Anwar, J. Am. Chem. Soc. 128 (2006) 13982-13983.
909 [65] Z.-W. Yu, P. J. Quinn, Mol. Membr. Biol.15 (1998) 59-68.
910 [66] C. N. Dolan, R. D. Moriarty, E. Lestini, M. Devocelle, R. J. Forster, T. E. Keyes, J. Inorg. Biochem. 119
911 (2012) 65-74.
912 [67] M. A. Randhawa, Jpn. J. Med. Mycol. 47 (2006) 314-318.
913 [68] B.M. Ghajar, S. A. Harmon, Biochem. Biophys. Res. Commun. 32 (1968) 940-944.

914 [69] H. C. Ansel, W. P. Norred, I. L. Roth, J. Pharm. Sci. 58 (1969) 836-839.
915 [70] E. Goemaere, A. Melet, V. R. Larue, A. l. Lieutaud, R. A. De Sousa, J. Chevalier, L. Yimga-Djapa, C.
916 Giglione, F. Huguet, M. Alimi, J. Antimicrob. Chemother. 67 (2012) 1392-1400.
917 [71] M. E. Hossain, M. N. Alam, J. Begum, M. Akbar Ali, M. Nazimuddin, F. E. Smith, R. C. Hynes, Inorg.
918 Chim. Acta 249 (1996) 207-213.
919 [72] J. A. Lessa, D. C. Reis, J. G. Da Silva, L. T. Paradizzi, N. F. Da Silva, M. De Fàtima A. Carvalho, S. A.
920 Siqueira, H. Beraldo, Chem. Biodivers. 9 (2012) 1955-1966.
921 [73] J. M. Bolla, S. Alibert-Franco , J. Handzlik, J. Chevalier, A. Mahamoud, G. Boyer G, K. Kiec-
922 Kononowicz, J.-M. Pagès, FEBS Lett. 585 (2011) 1682-1690.
923 [74] T. Mosmann, J. Immunol. Methods 65 (1983) 55-63.
924 [75] Z. Afrasiabi, E. Sinn, S. Padhye, S. Dutta, S. Padhye, C. Newton, C. E. Anson, A. K. Powell, J. Inorg.
925 Biochem. 95 (2003) 306-314.
926 [76] E. Pradel, J.-M. Pages, Antimicrob. Agents Chemother. 46 (2002) 2640-2643.
927 [77] M. Viveiros, A. Jesus, M. Brito, C. Leandro, M. Martins, D. Ordway, A. M. Molnar, J. Molnar, L. Amaral,
928 Antimicrob. Agents Chemother. 49 (2005) 3578-3582.
929 [78] P. Plesiat, H. Nikaido, Mol. Microbiol. 6 (1992) 1323-1333.
930 [79] G. W. Kaatz, S. L. Barriere, D. R. Schaberg, R. Fekety, J. Antimicrob. Chemother. 20 (1987) 753-758.
931 [80] V. Kuete, S. Alibert-Franco, K. Eyong, B. Ngameni, G. Folefoc, J. Nguemeving, J. Tangmouo, G. Fotso, J.
932 Komguem, B. Ouahouo, Int. J. Antimicrob. Agents 37 (2011) 156-161.
933 [81] G.M. Sheldrick, SADABS. University of Göttingen, Germany (1996).
934 [82] CrysAlis PRO, Agilent Technologies, Yarnton, Oxfordshire, England (2011).
935 [83] G.M. Sheldrick, Acta Crystallogr. Sect. C, 71 (2015) 3-8.
936 [84] L. J. Farrugia, J. Appl. Crystallogr. 32 (1999) 837-838.
937 [85] J. Gans, D. Shalloway, J. Molec. Graphics Model. 19 (2001) 557-559.
938 [86] K. Brandenburg, DIAMOND. Crystal Impact GbR, Bonn, Germany (2006).
939